Establishing a Neutronics Design and Equilibrium Cycle Analysis for the I^2S-LWR Reactor with UO_2 and U_3Si_2 Fuel

Andrew M. Ward[a,*], Ryan P. Hon[b], Gabe Kooreman[b], David Salazar[c], Fausto Franceschini[c], Thomas J. Downar[a]

[a] *Nuclear Engineering, University of Michigan,2355 Bonisteel Blvd, Ann Arbor, Michigan*
[b] *Nuclear Engineering, Georgia Institute of Technology, 770 State St, Altlanta, Georgia*
[c] *Westinghouse Electric Company, 1000 Westinghouse Dr, Cranberry Township, Pennsylvania*

Abstract

The Integral Inherently Safe (I^2S-LWR) reactor was developed not only to enhance passive reactor safety performance, but also to improve reactor economics. This paper describes the steady-state and depletion analysis of the I^2S-LWR core using both UO_2 and U_3Si_2 fuel designs. The development and validation of the core models are described, to include the generation of HELIOS cross sections and comparison with the WEC lattice code PARAGON and the Monte Carlo code SERPENT. The few group homogenized cross sections were then prepared for the U.S. NRC PARCS core simulator using the GenPMAXS code. The multicycle capability in PARCS was used to determine the equilibrium core condition for three batch cores loaded with the UO_2 and then with the U_3Si_2 fuel designs. Comparisons with the results from the WEC code ANC at beginning, middle, and end of cycle showed good agreement. Core conditions at beginning and end of cycle were then used to determine the converged steady-state conditions of a coupled RELAP5/PARCS model, which provided the initial condition for various transient accident simulations which are reported in a companion paper.

Keywords: I^2S-LWR, Modular, Inherent

*Corresponding author
Email address: wardam@umich.edu (Andrew M. Ward)

Preprint submitted to Annals of Nuclear Energy *May 9, 2018*

1. Introduction

Even prior to the event at Fukushima Daiichi in 2011, reactor vendor designs began to increase both the passive and inherent safety features of power reactors. These improvements generally were an evolution of the Gen-III LWR reactor resulting in several improvements in both safety and economic performance. An example of a Gen-III+ design would be the WEC AP-1000 reactor. However, a more revolutionary rethinking of the LWR design reactor was also considered and the fundamental plant design was re-envisioned resulting in a more integral reactor configuration. Examples of these new designs would include WEC SMR and the NuScale Power Module which have several features which provide improved passive safety and which utilize more economical approaches for design, construction, and operation.

This approach was extended to a comprehensive redesign of the conventional PWR in the form of the IRIS reactor concept which was first presented in 2002[1]. This concept subsequently evolved to what would become the I^2S-LWR reactor concept[2]. The I^2S-LWR was designed to accomplish several goals, with the most important being improved safety performance. By integrating the Nuclear Steam Supply System (NSSS) into the reactor vessel, which also increases in-core water inventory, the risk for a loss of coolant accident was significantly reduced. The second goal was to take advantage of as many advanced and novel technologies as possible, for example, wireless instrumentation and control, micro-channel heat exchangers, and steam drums. The final goal was to achieve a more cost effective design by reducing fuel and operating costs which increase plant economics.

The focus of this paper is the development of the core neutronics model for a core design with UO_2 and U_3Si_2 fuel options. Several well-established analysis tools will be used in the analysis presented in this paper. The neutron cross sections needed for fuel depletion were generated with the HELIOS lattice physics code[3]. The U.S. NRC reactor core neutronics simulator PARCS[4] was used to calculate the core neutronics solution for both steady-state and transient conditions, as well as to fuel cycle depletion calculations. The systems thermalhydraulics code RELAP5[5] was used to model the plant thermal-hydraulics and the coupled codes RELAP5/PARCS were used to calculate stable coupled solutions to the steady state simulation for use in the coupled transient analysis. Fuel and core design information can be found in an earlier publication [6], which was used throughout the following sections.

2. Cross Section Generation

2.1. Fuel Cross Section Modeling

The I^2S-LWR core was developed by WEC with both UO_2 and U_3Si_2 fuel options. Both fuel types use the same 19 x 19 pin assembly design. The general parameters for the assembly can be found in Table 1. The only difference between the two assembly designs is the size of the fuel pellet. The U_3Si_2 fuel pellet is annular shaped to allow more room for swelling. An illustration of the assembly layout is given in Figure 1.

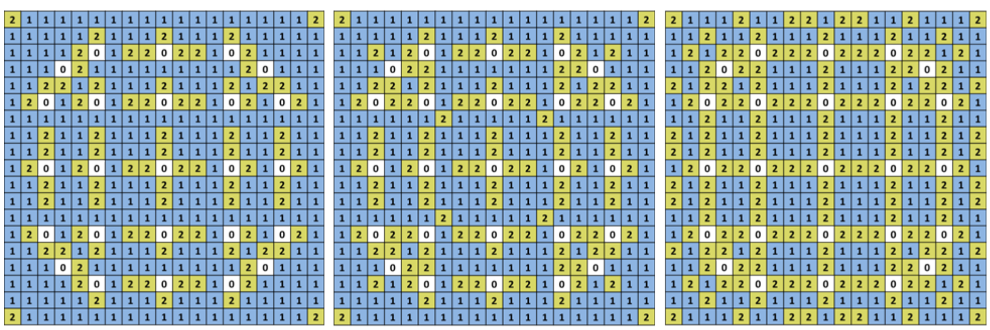

Figure 1: IFBA Fuel Pin Layout: 84 IFBA (left), 100 IFBA (center), 156 IFBA (right)
Legend: central 0 is instr. tube, 0s are guide tubes, greater than 0 are fuel pins

2.1.1. UO_2 Fueled Core

The UO_2 option has 2 unique assembly types, each split into 5 axial regions. Unlike the U_3Si_2 design, the fuel pellets in the UO_2 core are solid except for in

Table 1: Assembly Parameters

Assembly Type	19 x 19	-
Number of fuel pins	336	-
Number of guide / instrument tubes	25	-
Assembly Pitch	23.204	cm
Pin cell pitch	1.215	cm
Guide tube outer radius	0.548	cm
Instrument tube outer radius	0.555	cm
Guide / instrument tube inner radius	0.510	cm
Control rod clad radius	0.445	cm
Control radius	0.398	cm
UO2 fuel pellet outer radius	0.410	cm
UO2 fuel pellet inner radius	0.198	cm
U3Si2 fuel pellet outer radius	0.404	cm
U3Si2 fuel pellet inner radius	0.128	cm
IFBA loading	2.505	mg/in

the blanket region where it is annular to provide room for fission gases. The IFBA rod locations can be found in Figure 1. The unique assembly region types for the core are as follows:

- Blanket enriched to 2.60 wt% U-235 (annular)
- Cutback enriched to 4.80 wt% U-235
- Center fuel with 84 IFBA pins and enriched to 4.80 wt% U-235
- Center fuel with 156 IFBA pins and enriched to 4.80 wt% U-235

2.1.2. U_3Si_2 Fueled Core

The U_3Si_2 I^2S-LWR core design has four unique assembly types which vary with the enrichment and the number of pins with the IFBA coating. Each of these assembly types has five different axial regions, namely, a central fuel region with IFBA that encompasses most of the height of the pin, a bottom, and top cutback region (the IFBA coating is cut back) with the same enrichments as the central region, and a bottom, and top blanket with reduced fuel enrichment. Taking into account both axial and assembly variation, there are seven unique assembly regions:

- Blanket enriched to 2.60 wt% U-235
- Cutback enriched to 4.45 wt% U-235
- Cutback enriched to 4.65 wt% U-235
- Center fuel with 84 IFBA pins and enriched to 4.45 wt% U-235
- Center fuel with 156 IFBA pins and enriched to 4.45 wt% U-235
- Center fuel with 84 IFBA pins and enriched to 4.65 wt% U-235
- Center fuel with 100 IFBA pins and enriched to 4.65 wt% U-235

2.2. Nuclear Data Generation for PARCS

The lattice depletion code HELIOS version 1.10 was used to generate the nuclear data libraries for PARCS calculations. HELIOS is a general geometry lattice depletion code that uses current coupling and collision probabilities in 2D geometry. The code has been widely used and verified for both light and heavy water reactors.

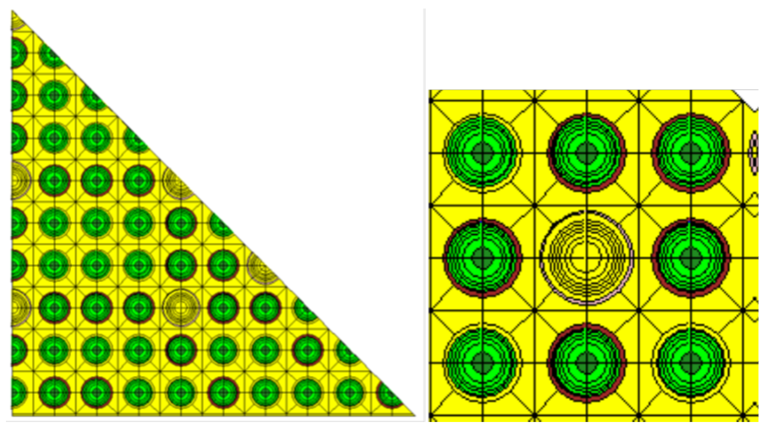

Figure 2: $1/8^{th}$ HELIOS model of a U_3Si_2 assembly with IFBA

For each of the seven unique assembly regions in the U_3Si_2 design and four unique assembly regions in the UO_2 design, a HELIOS transport model was constructed. The model was simplified to decrease the computation time in three ways. First, the $1/8^{th}$ symmetry of the assemblies was used in order to decrease the size of the transport problem. Next, current coupling was used on the pin cell boundaries instead of exact coupling, and finally, the assembly was meshed as shown in Figure 2. The use of current coupling and choice of mesh was shown to have a small effect on the result of the problem (less than 250 pcm on the eigenvalue) and was deemed acceptably accurate for the purposes of data generation. From Figure 2, it can be seen that the fuel and control material are divided into five radial and four azimuthal regions. The cladding is split into four azimuthal regions and is also smeared into the gap while preserving the total amount of material. The moderator around the pin cell is then split into eight regions with a small sliver of moderator region accounting for the inter assembly gap.

Table 2: History State Parameters

Control Rod State	Coolant Density (g/cm3)	Boron Concentration (ppm)	Coolant Temperature (K)	Fuel Temperature (K)
out	0.6081	500	585	800
out	0.7005	0.5	585	800
out	0.7005	500	585	555
out	0.7005	500	585	800
out	0.7005	500	585	1600
out	0.7005	1500	585	800
out	0.7697	500	585	800
in	0.7005	500	585	800

PARCS uses the word "history" to describe the TH conditions of the model during depletion. "Branches" describes the instantaneous state, where the TH conditions are varied but the fuel nuclide vector is held constant. Lattice calculations were performed to create XS data libraries for each unique assembly region. For each region, eight main histories were calculated corresponding to the reactor state parameters in Table 2, and the burnup points in Table 3. As seen in the tables, the coolant density, boron concentration, coolant temperature, fuel temperature and control state (rods in: 1, rods out: 0) were varied for each history calculation. For each of these histories, at each burnup point, 99 branch-off calculations were performed that vary the state parameters. These branch case state parameters were chosen so that data encompasses transient situations with cases having low moderator density situations (0.1 g/cm3), hot fuel (2800 K) and/or elevated soluble boron (2500 ppm). For all cases, macroscopic cross sections, microscopic cross sections for xenon, samarium and boron,

Table 3: Lattice Depletion Steps [MWd/tHM]

250	500	1000	1500	2000	2500	3000	3500
4000	4500	5000	5500	6000	6500	7000	7500
8000	8500	9000	9500	10000	11000	12000	13000
14000	15000	16000	17000	18000	19000	20000	22500
25000	27500	30000	32500	35000	37500	40000	42500
45000	47500	50000	52500	55000	57500	60000	62500
65000	67500	70000					

and delayed neutron parameters were output for use in PARCS safety calculations.

2.3. Validation of Lattice Results

In order to validate the data library generated by HELIOS, assembly lattice results were generated and then compared to data generated by Westinghouse (WEC) from their Paragon code [7]. These tests included pin cell and assembly depletion cases for both U_3Si_2 and UO_2 fuel. The tests included variation in the fuel temperature, soluble boron concentration, burnup, IFBA loading, and the presence of the B1 spectral correction. For these cases, Georgia Tech generated results with HELIOS while WEC generated results using their lattice physics code Paragon and the stochastic code Serpent [8].

One major difference between the HELIOS and Paragon codes is the data library used. The HELIOS library is based off of various ENDF/B-VI revisions (0, 1, 2, and 3) while Paragon was run with libraries based off of ENDF/B-VI.3. The different data libraries caused HELIOS to predict a higher eigenvalue (k-infinity) than Paragon, where the maximum difference was about 300 pcm, but most cases differed by around 200 pcm.

Another difference is the modeling of IFBA in the HELIOS model compared to that of Paragon. HELIOSv1.10 has a minimum size requirement for material regions, and thus is unable to correctly model the thickness of the IFBA coating on the fuel. In order to remedy this, IFBA was spread out into the gap up to the limit set by HELIOS while conserving the total amount of material. Sensitivity studies were performed on this smearing of IFBA into the gap and errors were found to be small (less than 100 pcm). Figures 3 through 6 present a summary of the data obtained from the various validation tests performed.

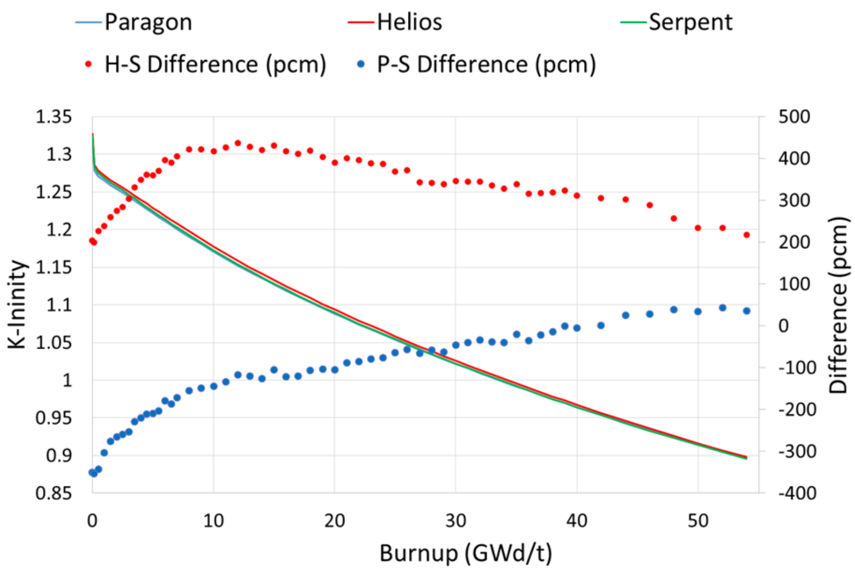

Figure 3: Paragon, HELIOS, and Serpent k-infinity results (left axis) for a U_3Si_2 pin with a fuel temperature of 900K. Difference (pcm) between Serpent and Helios and Serpent and Paragon presented as a scatter plot (right axis)

Figure 3 shows U_3Si_2 pin cell depletion results for Paragon, Helios, and Serpent. The lines represent the depletion curve for all three codes and the value of k-infinity is shown on the left axis. Serpent, using ENDF/B-VII, was used as a baseline of comparison between the code because 1) newer ENDF libraries are believed to be more accurate, and 2) Monte Carlo methods should give a more precise solution. The differences (in pcm) between Helios and Serpent as well as Paragon and Serpent are plotted as a scatter plot against the right axis. Serpent results are included to As seen in Figure 3 , HELIOS overestimates the eigenvalue when compared to Serpent over the whole depletion while Paragon first underestimates and then approaches the Serpent result towards the end of the depletion. A similar trend was seen in the UO_2 pin cases.

Figures 4 through Figure 6 show assembly level eigenvalue results for both Paragon and HELIOS. Figure 4 shows the case of a UO_2 assembly with 156 IFBA rods and a fuel temperature of 900K. Differences between HELIOS and Paragon are large at low burnups (less than 5 GWd/t) and are small at high burnups.

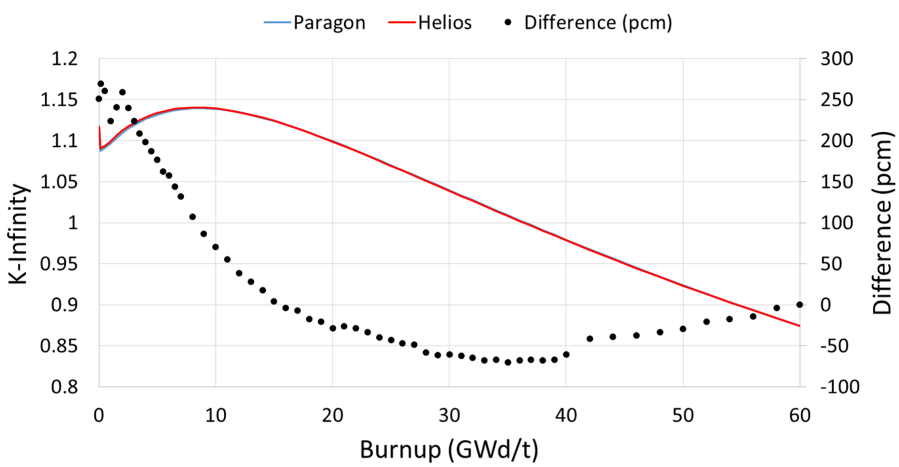

Figure 4: Paragon and HELIOS results for an UO_2 assembly with 156 IFBA pins with a fuel temperature of 900K, no boron

Figure 5 shows a similar case to the one in Figure 4 except for the presence of 2000 ppm of soluble boron. The general trend of the difference between Paragon and HELIOS is similar, with the largest difference at the beginning of the cycle and then decreasing. The presence of the soluble boron caused a shift in the difference of the eigenvalue by 200 pcm. Even though this causes a difference of between 250-450 pcm between the Paragon and HELIOS results, these differences are still relatively small. Since 2000 ppm of soluble boron is much higher (by 500pcm) than one would expect in normal operation conditions this effect is not as pronounced in further calculations.

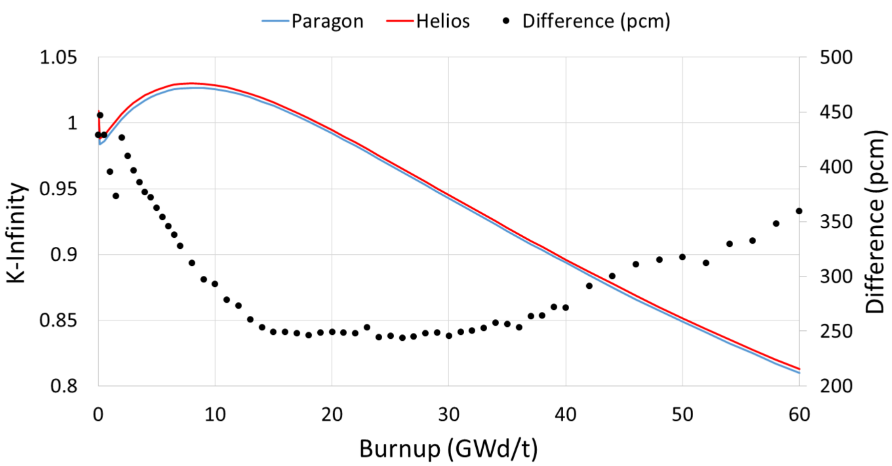

Figure 5: Paragon and HELIOS k-infinity results (left axis) for a UO_2 assembly with 156 IFBA pins with a fuel temperature of 900K and a soluble boron concentration of 2000 ppm. Difference between HELIOS and Paragon presented as a scatter plot

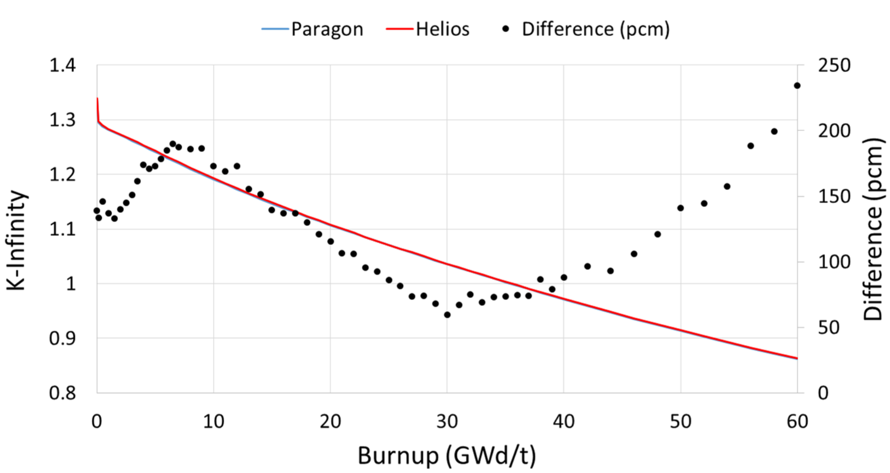

Figure 6: Paragon and HELIOS results for an U_3Si_2 assembly with a fuel temperature of 900K

Figure 6 shows an U_3Si_2 assembly case without the presence of IFBA. As with the UO_2 cases HELIOS calculates a slightly higher eigenvalue than does Paragon. Differences for this case between Paragon and HELIOS are below 250 pcm. Compared with Figure 3, the difference between Paragon and HELIOS is lower, which implies some beneficial cancellation of erros when moving from the pin cell to the assembly.

The differences between HELIOS and Paragon calculations have been quantified. The differences were seen to be small with some variation in the presence of soluble boron or burnable absorbers. The benchmark results give confidence that the data libraries generated by HELIOS for PARCS are similar to the ones generated by Paragon for ANC. Industry state-of-practice uses a 300 pcm limit for acceptance, and although the differences observed here are closer to 500 pcm, they are still belived to be acceptable at this stage of the safety analysis.

2.4. Reflector Modeling

Cross sections for the I^2S-LWR neutron reflector were also generated in HELIOS for PARCS calculations. However, the steel neutron reflector surrounding the reactor core does not yet have a finalized design. It is therefore necessary to construct an approximate model of the reflector in order to accommodate neutronics calculations on the whole core. The final design of the reflector will depend largely on thermohydraulic concerns including the gamma heating of the reflector steel, but the basic design will be a solid steel barrel with circular cooling channels.

Reflector cross sections were generated for a highly simplified homogenized model composed of 70% steel by weight. Cross sections were calculated using the HELIOS transport code. The transport model included a large reflector region alongside a single fresh fuel I^2S-LWR assembly with reflected boundary conditions on the three sides that are not outside the reflector, as shown in Figure 7. While this geometry does not adequately model the whole-core flux profile within the reflector, it is assumed to be a sufficient model for determining the neutron energy spectrum in the reflector. In order to accommodate PARCS calculations, reflector cross sections were generated for the several values of moderator density and boron concentration, which can be found in Table 4. This model was used to generate XS benchmark, depletion, and transient scenarios.

Figure 7 shows the reflector model with reflected boundary conditions at the top, left, and bottom and a vacuum boundary condition at the right side. On the left is a single fuel assembly (with 156 IFBA and 4.65% enrichment of U_3Si_2) and on the right is a large homogenized reflector region. The chosen composition of the reflector is far from what the actual composition of the I^2S-LWR reflector will be, as 70% steel by weight is only a thin mesh of steel. The initial investigation of the I^2S-LWR reactor used 70% steel by weight; this was a very conservative estimate to the actual reflector composition. In future work, this value will be changed to 70% steel by volume in order to more closely match the expected composition of the reflector.

Table 4: Reflector XS branch calculations

Water Densities (g/cm3)	Boron Concentrations (ppm)
0.05	0.1
0.2	650
0.4	1300
0.6	1900
0.8	2600

3. Steady State Neutronics

The I^2S-LWR is designed to use an accident tolerant fuel, but can be operated with a standard UO_2/Zirc fuel as well. The two fuel designs which were applied in this paper are the annular U_3Si_2/SS fuel as well as the conventional UO_2/Zirc. All core management, loading, and depletion calculations were

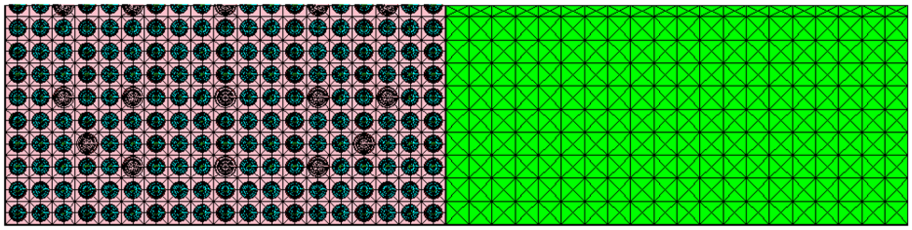

Figure 7: HELIOS Reflector Model

performed by Westinghouse Electric Company. Comparisons were made with PARCS in order to both confirm the calculations performed by ANC [9] and also to utilitze the RELAP5/PARCS system for coupled transient simulations.

The core configuration of the I^2S-LWR is very similar to that of a Westinghouse 2-Loop, with 121 fuel assemblies. Various cycle lengths and loading patterns were explored, but the 18 month-3 batch cycle will be considered in this paper. Fuel designs and loading patterns were developed by Westinghouse Electric Company, with previously published results [6] used as the basis for the comparison.

3.1. Core Depletion

The core configuration for both the UO_2 and U_3Si_2 options are given in Figure 8. As can be seen the layout is generally checkerboard with a 4th batch used for the central assembly.

The depletion methodology in PARCS is a continuous, generic multicycle approach. Fuel is depleted in a specified configuration until a predetermine number of steps have been completed. The step lengths, control state, and thermal-hydraulic conditions can be adjusted between steps. After the final step, the fuel is shuffled. This shuffling allows for burned fuel to be moved about the core individually or via batches, while fresh fuel can also be added. A spent fuel pool option is also available. An illustration is given in Figure 9.

Following the multicycle approach described in the earlier section, an equilibrium core was developed. The approximate cycle length of 18 months was accomplished by taking 18 one month steps. At the end of the cycle, the shut-

	G	F (H)	E (J)	D (K)	C (L)	B (M)	A (N)
7	3X K-2 38737 40665	1X L-5 17680 18489	Feed 4.65/4.80 100 - 2.5 156 - 2.5	2X E-9 33369 35062	1X B-7 17263 18565	Feed 4.65/4.80 84 - 2.5 84 - 2.1	2X L-7 34554 36651
8 (6)	1X E-3 17680 18489	2X D-10 33416 34496	1X F-3 18860 20122	1X H-2 15829 16980	Feed 4.45/4.80 156 - 2.5 156 - 2.5	Feed 4.65/4.80 84 - 2.5 84 - 2.1	2X D-9 31293 33608
9 (5)	Feed 4.65/4.80 100 - 2.5 156 - 2.5	1X C-6 18854 20114	1X E-11 17681 18486	1X L-4 14436 15808	Feed 4.45/4.80 84 - 2.5 156 - 2.5	2X H-9 33944 35795	
10 (4)	2X J-9 33369 35062	1X M-6 15829 16981	1X K-3 14421 15789	1X G-5 17503 17490	Feed 4.45/4.80 84 - 2.5 84 - 2.1	2X D-8 32672 34338	
11 (3)	1X G-12 17263 18565	Feed 4.45/4.80 156 - 2.5 156 - 2.5	Feed 4.45/4.80 84 - 2.5 156 - 2.5	Feed 4.45/4.80 84 - 2.5 84 - 2.1	2X G-8 31097 32332		
12 (2)	Feed 4.65/4.80 84 - 2.5 84 - 2.1	Feed 4.65/4.80 84 -2.5 84 -2.1	2X E-6 33943 35794	2X F-10 32661 34325		1X L-5 17680 18489	Times Burned Previous Core Location BOC BU U_3Si_2 Core BOC BU UO_2 Core
13 (1)	2X G-3 34554 36651	2X E-10 31287 33598				Feed 4.65/4.80 100 - 2.5 156 - 2.5	Fresh Fuel ^{235}U w/o U_3Si_2/UO_2 Core # IFBA - ^{10}B mg/in U_3Si_2 Core # IFBA - ^{10}B mg/in UO_2 Core

Figure 8: I^{2}S-LWR Core Loading

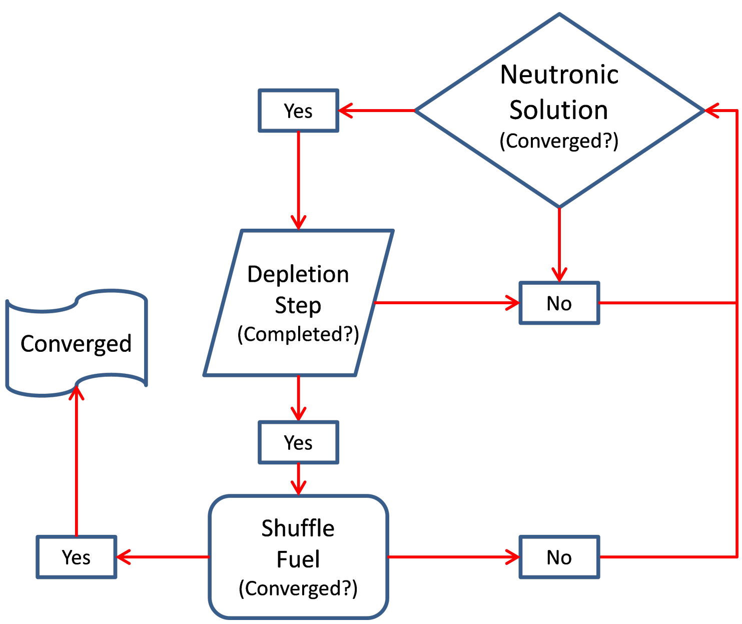

Figure 9: PARCS Multicycle Search Flowchart

down is approximated by two zero power steps prior to the shuffle. A simple mass-energy solver is used to provide TH feedback to the neutronic and depletion calculation. The boron letdown curve, radial power shape, and axial peak power are compared for several steps in the following section.

The boron letdown curve is given for the UO_2 and U_3Si_2 core in Figure 10 and Figure 11. The most notable differences from ANC are in the first two points. This is likely related to the treatment of Xe/Sm for 0 burnup fuel assemblies. During the first depletion step, there is reduced Xe/Sm, but PARCS provides a small amount of burnup to the fuel to allow a realistic Xe/Sm concentration. This treatment differs between ANC and PARCS. Generally, the boron concentration agrees very well. The boron difference for the first point was excluded as the Xe/Sm treatments are different, and the value would have dwarfed the other differences.

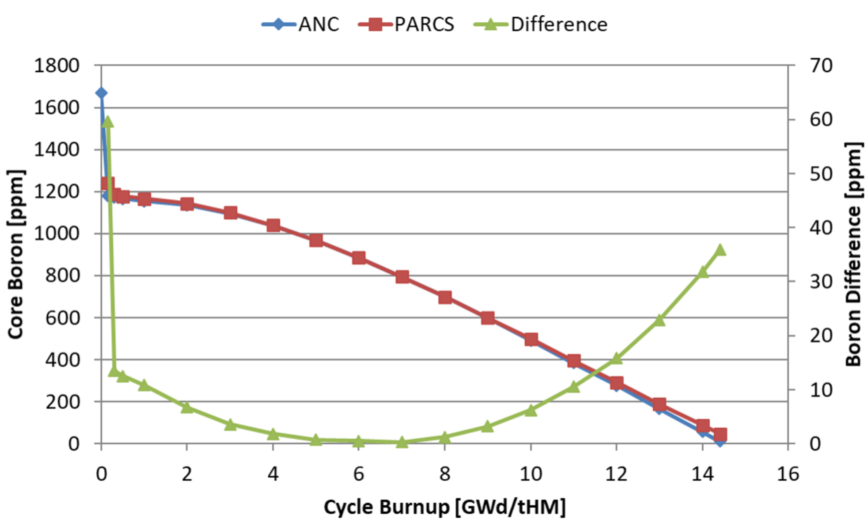

Figure 10: UO_2 Core Boron Letdown

The radial power shapes were compared at the beginning (BOC) and end of the cycle (EOC). Results for the UO_2 core are given in Figure 12 and Figure 13.

The agreement in the power shapes is generally good, however, some slgith

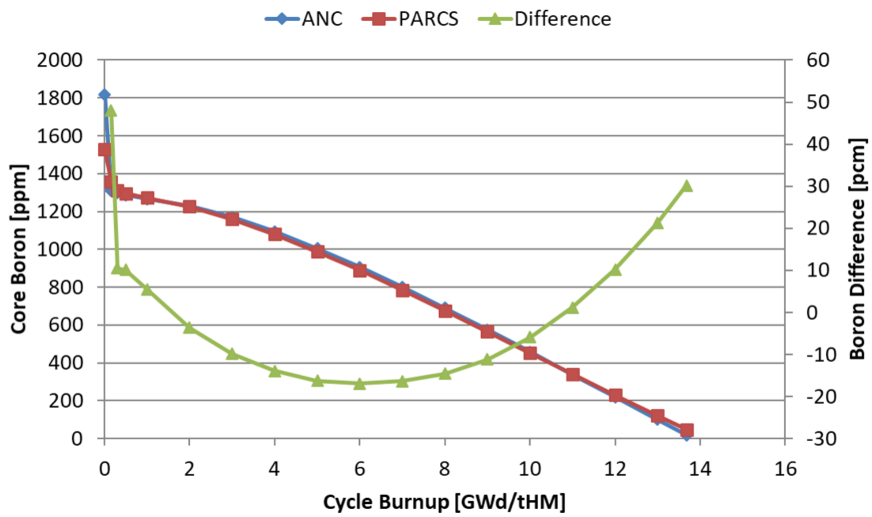

Figure 11: U_3Si_2 Core Boron Letdown

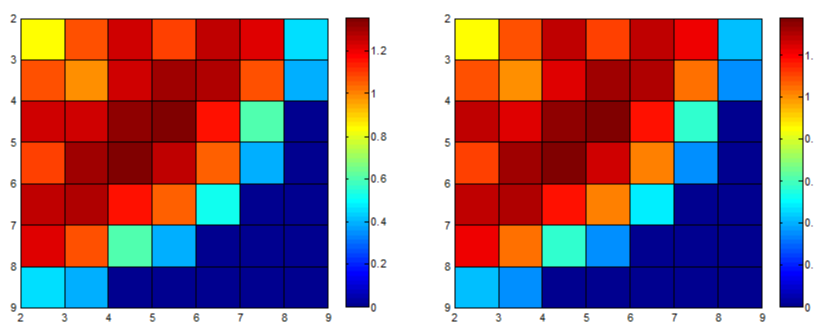

Figure 12: UO_2 Core Radial Power, BOC
ANC(left), PARCS(right)

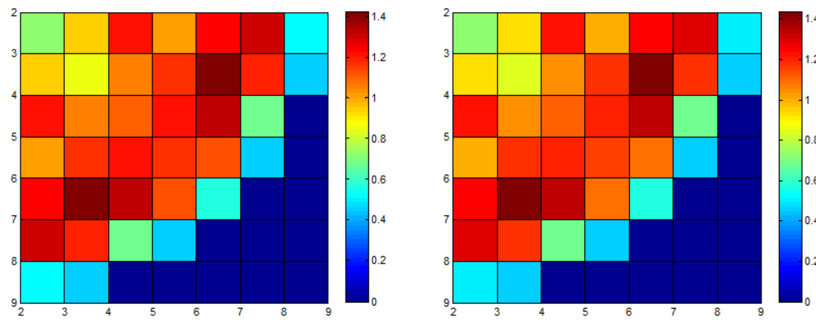

Figure 13: UO_2 Core Radial Power, EOC
ANC(left), PARCS(right)

differences can be observed near the periphery which results primarily from different reflector treatment. This can be seen across the entire cycle which suggests the difference is systematic. Efforts are underway to implement an option that would enable a consistent reflector treatment in PARCS. Results for the U_3Si_2 core are given in Figure 14 and Figure 15. The boron difference for the first point was excluded as the Xe/Sm treatments are different, and the value would have dwarfed the other differences.

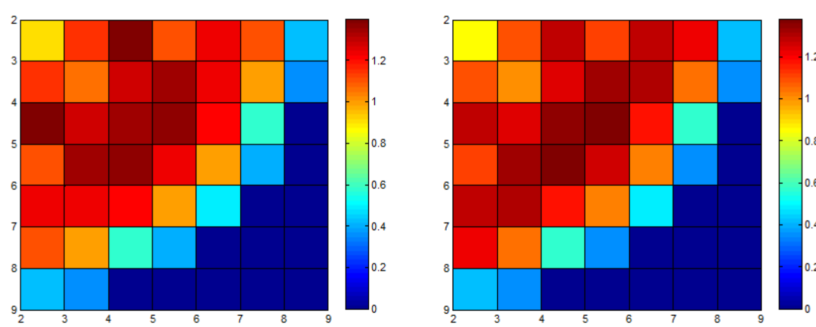

Figure 14: U_3Si_2 Core Radial Power, BOC
ANC(left), PARCS(right)

Again, there is good agreement between ANC and PARCS with similar differences observed near the periphery. The peak axial power is provided in Figure

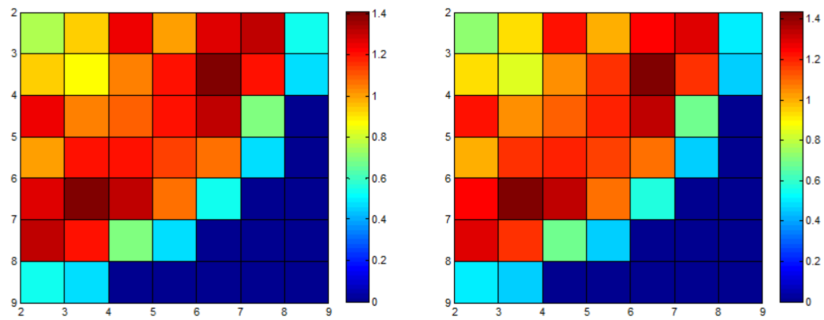

Figure 15: U_3Si_2 Core Radial Power, EOC
ANC(left), PARCS(right)

16 and Figure 17. Similar to the boron letdown, the 0 burnup point differs significantly. However, the remaining points show very good agreement.

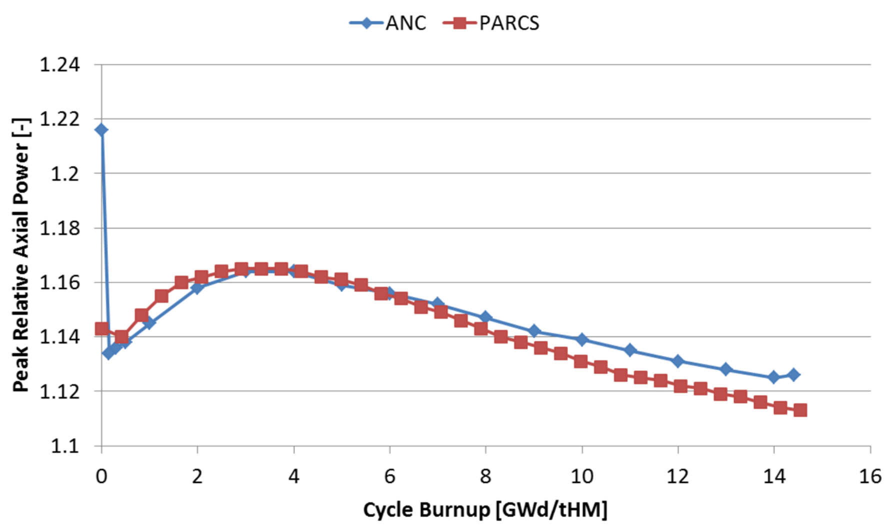

Figure 16: UO_2 Core Axial Peak Throughout Cycle

Again, aside from the 0 burnup point, very good agreement was observed across the cycle. The axial power in the U_3Si_2 is slightly higher than the UO_2 core until about 5 GWd/tHM, then it is lower. The above results provide confidence in the initial state used for the transient calculations. Transient cases

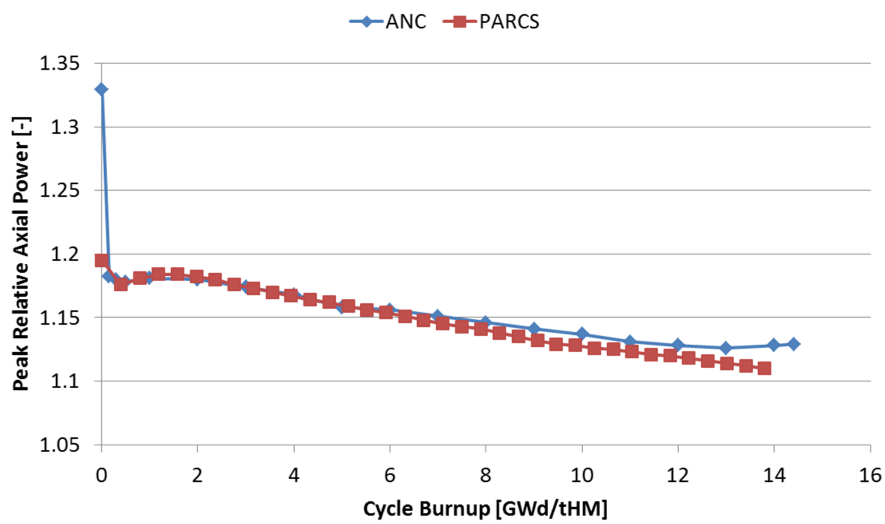

Figure 17: U_3Si_2 Core Axial Peak Throughout Cycle

will be performed at the same beginning and end of cycle states. Cold comparisons and reactivity coefficients were calculated for several cases. Agreement was acceptable, but the results were not given here for the sake of brevity.

4. Coupled System Thermal-Hydraulics and 3D Neutronics

A coupled systems thermal-hydraulics and 3D neutronics model was then developed for the I^{2}S-LWR reactor using the well-established RELAP5/PARCS code system which provides for steady state and time dependent calculations [10]. RELAP5 is capable of simulating the plant thermal-hydraulic behavior, and also coordinating feedback effects with PARCS which provides for the analysis of a wide range of complex system transients.

A steady state, or null transient, was used to obtain a coupled solution for the overall reactor condition. Generally, this coupled null transient requires 300-500 seconds of simulation time to obtain a stable solution. Different steady state cases are required for different burnup conditions, rod positions, or power levels.

A converged steady-state solution can be achieved with either one or two steps. If the one step procedure is used, the coupled case is executed directly and allowed to run until convergence. In the two step approach, RELAP5 is executed in standalone mode to provide a better initial guess for the coupled calculation. This RELAP5 data is then used to restart the coupled null transient. Although several different core conditions were subsequently used in the transient calculations, the convergence was similar in all cases. Although the core conditions are the primary focus in the coupled simulation, the balance of plant must be converged as well.

4.1. Thermal Hydraulic Convergence

The coupled plant modeled was run to about 300s of a null transient and convergence was monitored throughout the model. The Pressure is shown in Figure 18 for the upper and lower plenums and also the downcomer. The behavior indicates good convergence.

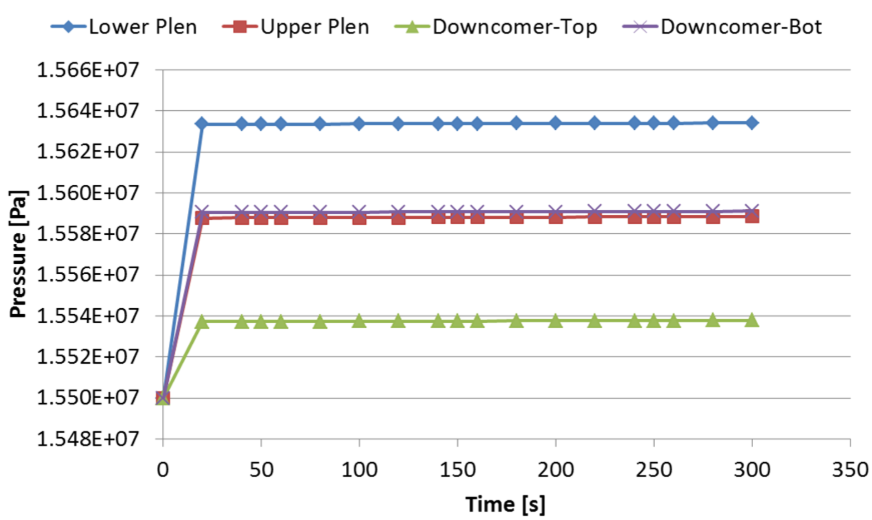

Figure 18: Coupled Steady State Pressure Convergence Plenum

The most sensitive location for convergence is generally in the core region, as the power is changing along with the thermal-hydraulic solution. Convergence appears to be stable with both fuels throughout the core and plant. Selected plots are given for the sake of brevity. Several core channels were checked to ensure good convergence. A channel group near the edge of the core is given in Figure 19. An example of the fuel heat structure convergence is given in Figure 20.

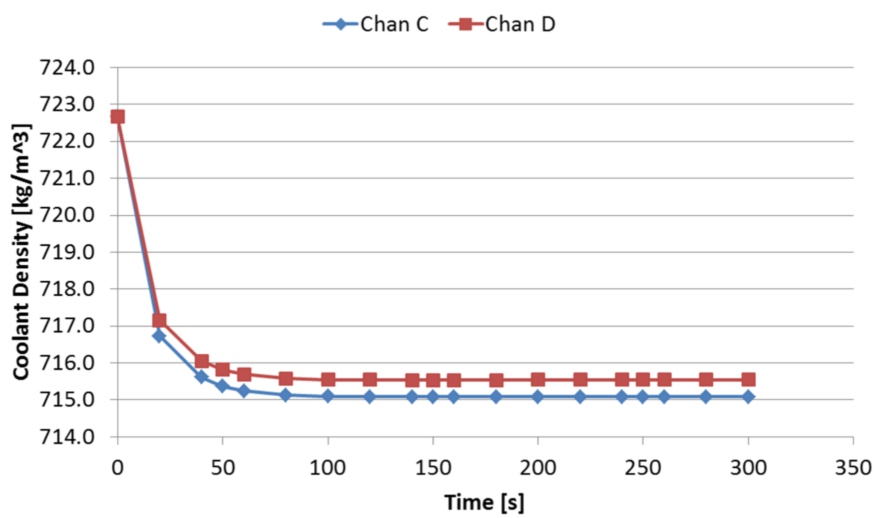

Figure 19: Coupled Steady State Outer Core Coolant Density Convergence

4.2. Neutronic Convergence

The Doppler temperature discussed here is taken as the linear combination of the heat structure centerline and surfaces temperatures. Neutronic convergence was determined by monitoring several parameters, to include the fission source, the boron concentration, and the change in the Doppler temperature. The Doppler change is shown in Figure 21. The simulation time represents the time scale used by RELAP5 during its null transient.

The fission source and boron concentration are shown in Figure 22. The dependent variable is given as iterations, as there are several neutronic iterations per time step advance in RELAP5. Although the boron concentration stabilizes

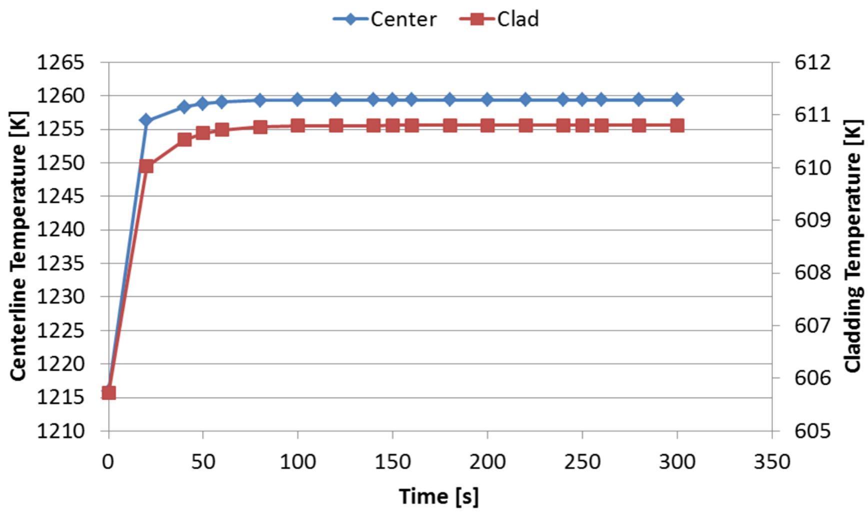

Figure 20: Coupled Steady State Inner Core Fuel Temperature Convergence

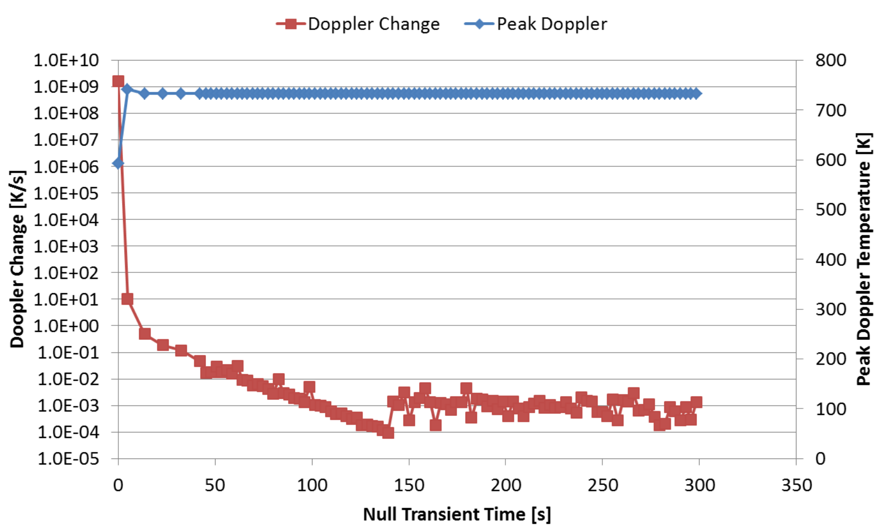

Figure 21: Coupled Steady State Doppler Convergence

quickly, the fission source converges more slowly. This results from the variations in the power shape as the coupled solution converges.

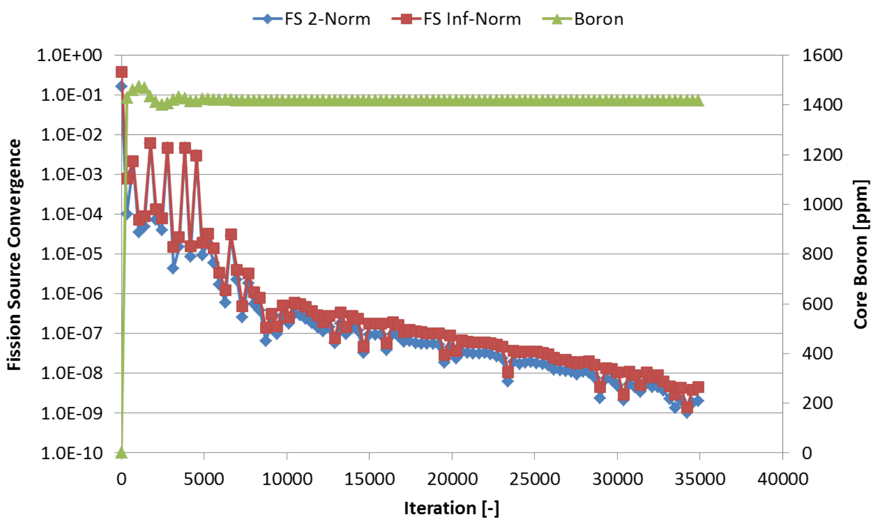

Figure 22: Coupled Steady Fission Source Convergence

5. Conclusions

This paper described the neutronics design and equilibrium cycle depletion of the Integral Inherently Safe (I^2S-LWR) reactor using both UO_2 and U_3Si_2 fuel types. The well established lattice physics code HELIOS was used to generate cross sections with appropriate parameterizations for history and instantaneous effects for core depletion using the U.S. NRC core simulator PARCS. Reflector cross sections were also developed using the conventional fuel+reflector model.

Comparisons between HELIOS and the WEC lattice code PARAGON indicated good agreement, with Serpent results were generated as well. HELIOS results were then processed through GenPMAXS for use in PARCS to perform multicycle depletion calculations. Comparisons with the WEC core simulator ANC showed acceptable agreement for both UO_2 and U_3Si_2 core designs. Core configurations from the BOC and EOC were used to establish initial conditions for the coupled code model developed using RELAP5/PARCS. Simulation of the steady state or null transient conditions with RELAP5/PARCS indicated stable solutions were achieved for both UO_2 and U_3Si_2 at BOC and EOC conditions. This converged core state provided the initial conditions for the transient conditions in the I^2S-LWR reactor.

References

[1] M. E. Ricotti, A. Cammi, A. Cioncolini, A. Cipollaro, F. Oriolo, C. Lombardi, L. E. Conway, A. C. Barroso, Preliminary safety analysis of the iris reactor, in: Proceedings of ICONE10, 2002.

[2] B. Petrovic, F. Rahnema, A. Manera, P. Ferroni, A. Haghighat, W. Hines, B. Upadhyaya, I. Charit, L. Muldrow, A. Ougouag, R. Cocherell, G. Parks, M. Ricotti, Integral inherently safe light water reactor (i2s-lwr) concept, in: Proposal to DOE NEUP, 2012.

[3] R. Stammler, J. Casal, A. Ferri, E. Villarino, User's Manual for HELIOS, Studsvik Scandpower (1994).

[4] T. Downar, Y. Xu, V. Seker, PARCS, U.S. NRC Core Neutronics Simulator, University of Michigan (2009).

[5] I. Information Systems Laboratories, RELAP5/MOD3 CODE MANUAL VOLUME IV: Models and Correlations (2001).

[6] D. Salazar, F. Franceschini, I2s-lwr equilibrium cycle core analysis, in: Physor 2014, 2014.

[7] M. Ouisloumen, H. Huria, H. Matsumoto, Paragon: The new westinghouse assembly lattice code, in: ANS Int. Mtg. on Mathematical Methods for Nuclear Applications, 2001.

[8] J. Leppnen, M. Pusa, T. Viitanen, V. Valtavirta, T. Kaltiaisenaho, The serpent monte carlo code: Status, development and applications in 2013, Annals of Nuclea 82 (2015) 142–150.

[9] L. Mayhue, R. Milanova, H. Huria, B. Zhang, E. Mller, F. Franceschini, M. Ouisloumen, P. F. Guimarae, Qualification of nexus/anc nuclear design system for pwr analyses, in: Physor, 2008.

[10] T. Kozlowski, R. Miller, T. Downar, H. Joo, D. Barber, Consistent comparison of the codes relap5/parcs and trac-m/parcs for the oecd mslb coupled code benchmark, Nuclear Tec.